# Mutations in *ATP2A2*, encoding a $Ca^{2+}$ pump, cause Darier disease

Anavaj Sakuntabhai[1], Victor Ruiz-Perez[2], Simon Carter[2], Nick Jacobsen[3], Susan Burge[4], Sarah Monk[1], Melanie Smith[2], Colin S. Munro[5], Michael O'Donovan[3], Nick Craddock[6], Raju Kucherlapati[7], Jonathan L. Rees[8], Mike Owen[3], G. Mark Lathrop[1], Anthony P. Monaco[1], Tom Strachan[2] & Alain Hovnanian[1]

**Darier disease (DD) is an autosomal-dominant skin disorder characterized by loss of adhesion between epidermal cells (acantholysis) and abnormal keratinization. Recently we constructed a 2.4-Mb, P1-derived artificial chromosome contig spanning the DD candidate region on chromosome 12q23–24.1. After screening several genes that mapped to this region, we identified mutations in the *ATP2A2* gene, which encodes the sarco/endoplasmic reticulum $Ca^{2+}$-ATPase type 2 isoform (SERCA2) and is highly expressed in keratinocytes. Thirteen mutations were identified, including frameshift deletions, in-frame deletions or insertions, splice-site mutations and non-conservative missense mutations in functional domains. Our results demonstrate that mutations in *ATP2A2* cause DD and disclose a role for this pump in a $Ca^{2+}$-signalling pathway regulating cell-to-cell adhesion and differentiation of the epidermis.**



## Introduction

DD, also known as Darier-White disease and keratosis follicularis (OMIM 124200), is a dominantly inherited skin disorder characterized by warty papules and plaques in seborrheic areas (central trunk, flexures, scalp and forehead), palmo-plantar pits and distinctive nail abnormalities[1] (Fig. 1*a*). The prevalence of the disease has been estimated at 1 in 55,000. Onset is usually before the third decade, and penetrance is complete in adults although expressivity is variable[2]. Involvement may be severe, with widespread itchy malodorous crusted plaques, painful erosions, blistering and mucosal lesions. Secondary infection is common. Sun, heat and sweating exacerbate the disease. DD never remits, but oral retinoids may reduce hyperkeratosis. DD has been reported to be associated with neuropsychiatric abnormalities including mild mental retardation and epilepsy in a few families[1]. The typical histological features include focal areas of separation between suprabasal epidermal cells (acantholysis), suprabasal clefting and unusual dyskeratosis (abnormal keratinization) with round dyskeratotic keratinocytes ('corps ronds'; Fig. 1*b*,*c*). Electron microscopy reveals loss of desmosomal attachments, perinuclear aggregations of keratin filaments and cytoplasmic vacuolization. These observations suggest that molecules which mediate adhesion between keratinocytes, such as the desmosomal cadherins (desmogleins and desmocollins) and desmosomal plaque proteins (desmoplakin, plakoglobin), or intermediate filament proteins might be involved in the loss of cell-cell adhesion in the epidermis[3]. Alternatively, the defect may lie in a molecule that regulates expression, recruitment, sorting or association of adhesion molecules.

DD has been linked to chromosomal region 12q23–24.1, initially within a 12-cM interval[4,5]. Subsequent linkage studies showed no evidence for locus heterogeneity, and the size of the critical region was reduced further to approximately 2 cM (refs 6–9). We analysed additional families, refined the DD region to an interval of less than 1 cM between *D12S1339* and *D12S2263* and constructed a 2.4-Mb YAC/PAC/BAC (P1-artificial chromosome/bacterial artificial chromosome) contig spanning the critical genetic interval[10].

We identified 12 genes in this interval using a combination of EST database searching, cDNA selection and sequence analysis of bacterial clones of the contig (http://gc.bcm.tmc.edu:8088/cgi-bin/seq/bcm-web-tables). We investigated these genes for expression in keratinocytes before screening them for mutations in DD patients. One of these genes, *ATP2A2,* encodes the sarco/endoplasmic reticulum $Ca^{2+}$-ATPase isoform 2 (SERCA2), a $Ca^{2+}$ pump that has a pivotal role in intracellular $Ca^{2+}$ signalling[11]. Together with the highly related SERCA1 and SERCA3 isoforms encoded by *ATP2A1* and *ATP2A3*, respectively, SERCA pumps belong to the large family of P-type cation pumps that couple ATP hydrolysis with cation transport across membranes. SERCA pumps specifically maintain low cytosolic $Ca^{2+}$ concentrations by actively transporting $Ca^{2+}$ from the cytosol into the sarco/endoplasmic reticulum lumen[12,13]. *ATP2A2* encodes two alternatively spliced transcripts, *ATP2A2a* (*HK2*) and *ATP2A2b* (*HK1*), encoding isoforms SERCA2a and SERCA2b, respectively. SERCA2a and SERCA2b differ in their carboxy-termini and have distinct tissue-expression patterns[11]. SERCA2a is primarily located in heart and slow-twitch skeletal muscle, whereas

[1]*The Wellcome Trust Centre for Human Genetics, University of Oxford, Oxford, OX3 7BN, UK.* [2]*Department of Human Genetics, University of Newcastle upon Tyne, NE1 7RU, UK.* [3]*Department of Psychological Medicine, University of Wales College of Medicine, Cardiff, CF4 4XN, UK.* [4]*Department of Dermatology, Churchill Hospital, Oxford, OX3 7LJ, UK.* [5]*Department of Dermatology, Southern General Hospital, Glasgow, G51 4TF, UK.* [6]*Department of Psychiatry, University of Birmingham, Birmingham, B152QZ, UK.* [7]*Department of Molecular Genetics, Albert Einstein College of Medicine, New York, New York 10461, USA.* [8]*Department of Dermatology, University of Newcastle upon Tyne, NE1 7RU, UK. Correspondence should be addressed to A.H. (e-mail: alain.hovnanian@well.ox.ac.uk) or T.S. (e-mail: tom.strachan@ncl.ac.uk).*

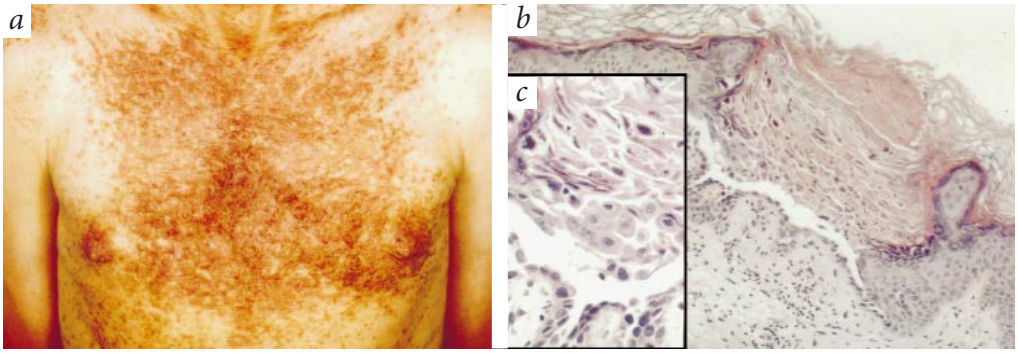


**Fig. 1** Clinical and histological features of Darier disease. ***a***, Clinical presentation of a patient with DD. Keratotic papules coalesce to form extensive plaques on the chest. ***b***, Histological section of affected skin showing separation of suprabasal cells ('acantholysis'), suprabasal cleft and abnormal keratinisation (×50). ***c***, Higher power showing acantholytic cells in the suprabasal layer (×100).

SERCA2b is present in smooth muscle and non-muscle tissues[14]. *ATP2A2* seemed a good candidate for DD because cytosolic $Ca^{2+}$ is known to have a role in the development of epithelial junctions and in regulating cell differentiation[15,16].

## Results

### Identification and mutation testing of putative candidate genes in the DD region

We performed EST database searches, direct cDNA selection and analysis of genomic sequence on bacterial clones spanning the critical region. We identified the following: a glycolipid transfer protein gene; *ATP2A2*; *ARC21* (also known as *ARP2/3*; encoding actin polymerization-related protein); a gene related to yeast *FET5* (encoding an ATP/GTP binding transcription factor); human U79274 (no homology with known proteins), a gene related to yeast *PEP11* (or *VPS29*; involved in vacuolar protein sorting); *RPL31* (encoding ribosomal protein L31), *PPM2C* (encoding protein phosphatase 2C); *PPP1CC* (encoding the protein phosphatase 1γ subunit), *RPL29* (encoding cell-surface heparin-binding protein); AI123295 (similar to cytoskeletal proteins) and *MYL2* (encoding myosin light chain 2). Among these genes, the glycolipid transfer protein gene and *ATP2A2* were found to be highly expressed in keratinocytes, as shown by northern-blot analysis, whereas transcripts of the others were detected only by RT-PCR. The glycolipid transfer protein gene, *ATP2A2*, *ARC21*, *PEP11*-related gene, *PPM2C*, *PPP1CC* and AI123295 were potential candidate genes on the basis of their known function or protein similarity. We performed mutation screening on these genes in DD patients and only identified defects in *ATP2A2*.

### Isoforms *ATP2A2a* and *ATP2A2b* are expressed in keratinocytes

We investigated the expression of *ATP2A2a* and *ATP2A2b* transcripts in keratinocytes by hybridizing northern blots containing keratinocyte RNA with probes *D12S2026* and *D12S1965*, which are specific for the 3′ untranslated end of the *ATP2A2a* and *ATP2A2b* isoforms, respectively. Each probe showed a 4.5-kb signal of strong intensity, indicating that both alternatively spliced transcripts of *ATP2A2* are expressed at high levels in cultured keratinocytes (Fig. 2*a*). The same probes were used to hybridize multiple-tissue northern blots (Fig. 2*b*). The hybridization results showed that *ATP2A2a* was strongly expressed in heart and skeletal muscle, as reported previously[11], but also revealed a larger transcript of approximately 6 kb in brain. This transcript is likely to correspond to the class 4 *ATP2A2* mRNA previously described as the main splice variant of *ATP2A2* in brain[17]. In contrast, an *ATP2A2b* transcript of weak intensity was detected in all tissues tested (data not shown).

### Genomic organization of *ATP2A2*

We used the genomic sequence generated from PAC 305I20 to determine the intron/exon boundaries of *ATP2A2*. We compared this sequence with the *ATP2A2* cDNA sequence using the BLAST2 sequence program from NBCI (http://www.ncbi.nlm.nih.gov/gorf/bl2.html) and identified the position and sequence of all introns of *ATP2A2* (Table 1). Of 21 exons, 19 were predicted using the programs GRAIL2, Genefinder, FGene and Genescan from the NIX program from HGMP (http://www.hgmp.mrc.ac.uk/NIX/). The gene spans approximately 76 kb, its smallest intron is 82 bp and its largest intron is 25.097 kb.

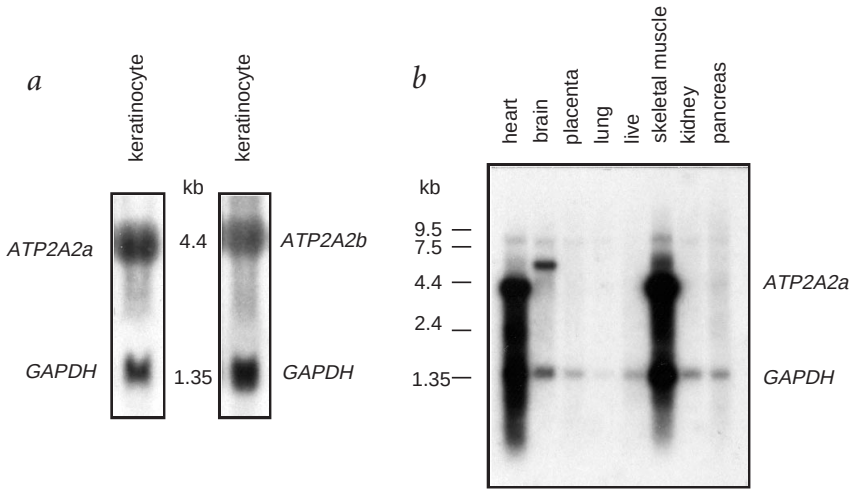


**Fig. 2** Tissue expression of the *ATP2A2* transcripts. **a**, Northern blots with human keratinocyte total RNA (30 μg) were hybridized with a PCR product generated with primers for *D12S2026* (specific for *ATP2A2a*) and *D12S1965* (specific for *ATP2A2b*). **b**, Multiple-tissue northern blot (Clontech) was hybridized with a PCR product generated with primers for *D12S2026*. Hybridizations with control *GAPDH* probe are shown.

**Table 1 • Intron-exon organization of the *ATP2A2* coding region**

| Exon/ intron | Exon length (bp) | Starting position in cDNA | Acceptor splice site[a] | Donor splice site[a] | Intron length (bp) |
|---|---|---|---|---|---|
| 1 | 118[b] | 1 | | CTCCAACG/gtaggtgcagggcgct | 696 |
| 2 | 18 | 119 | tttctacattctacag/AGTTACCG | TGAAGAAG/gtaatcttaacatgct | 91 |
| 3 | 83 | 137 | tgtttgtttcttacag/GAAAAACC | TATCTTTT/gtaagtataaaaaaat | 9,224 |
| 4 | 105 | 220 | gccatttctcttctag/GTTTTGGC | TATGGCAG/gtaagcaaaaattcct | 4,474 |
| 5 | 139 | 325 | gttttctttttatacag/GAAAGAAA | AATTGCTG/gtgagttgagtttgtc | 25,097 |
| 6 | 81 | 464 | tttttctcctaattag/TTGGTGACT | CTCACAG/gtaaatatgatatatt | 3,317 |
| 7 | 86 | 545 | ctcacaacccgcttag/GTGAATCT | TGTTTTCT/gtaagtactttatgaa | 1,077 |
| 8 | 465 | 631 | tctacttctgtcctag/GGTACAAA | TCTGCAGG/gtaagaggagtaattt | 4,579 |
| 9 | 89 | 1,096 | cgctctccccctacag/ATGTTCAT | GGAGAAGT/gtgagtaaccctcctc | 494 |
| 10 | 103 | 1,185 | ttttctctttgggcag/GCATAAAG | ACAATGAG/gtaagtctcttcataa | 728 |
| 11 | 132 | 1,288 | cctttaaccaatacag/GCAAAGG | GGCAACTCA/gtgagtatttgaacct | 5,137 |
| 12 | 123 | 1,420 | tttgttccctttgtag/GTCATTAA | TTGTGAAG/gcaagtatggcagatt | 99 |
| 13 | 219 | 1,543 | tctgtaacatttccag/GGTGCTCC | AATATGAG/gttagctaatgaaaag | 937 |
| 14 | 336 | 1,762 | gatgctcttattttag/ACCAATCT | CAGCTATG/gtgagcatgtttgaac | 1,233 |
| 15 | 221 | 2,098 | ttgctttccctttcag/ACTGGCGA | GTTGTCTG/gtaggtctctgtgaca | 783 |
| 16 | 203 | 2,319 | tcttgattggaaacag/TATTTTCC | TATTGGCT/gtgagtacaatttttt | 1,451 |
| 17 | 86 | 2,522 | ctgtgtttgttcccag/GTTACGTC | ACCAGCTG/gtactcagtcaccttt | 277 |
| 18 | 134 | 2,608 | ttggattttcttgcag/AGTCATTT | CTCAACAG/gttagtgcaccttcac | 618 |
| 19 | 118 | 2,742 | tctccttgctctgcag/CTTGTCCG | CCTTGCCA/gtaagtggttgggtgg | 82 |
| 20 | 267[c] | 2,860 | cttccctgtgtgtcag/CTCATCTT | GGAACCTGGTAAAGAGTGT[d] | 12,521 |
| 21 | 11[c] | 2,981 | tctctttcctttttcag/CAATACTG | | |

[a]The exonic and intronic sequences are indicated in uppercase and lowercase letters, respectively. [b]All coding sequence. [c]Down to stop codon. [d]This sequence, located in exon 20, is spliced at a GT cryptic donor splice (underlined) to generate the *ATP2A2a* isoform by joining exon 21 to the first 121 nt of exon 20. The *ATP2A2b* isoform contains the entire exon 20 and no exon 21 sequence[11].

## Mutations in *ATP2A2*

Extensive long-range restriction mapping, involving hybridization of ten different probes from the DD critical region to PFGE Southern blots of DNA samples from DD patients, showed no evidence of large-scale rearrangements. We hybridized Southern blots of genomic DNA from DD patients with cDNA probes spanning the entire *ATP2A2* coding region, but detected no abnormal restriction fragments. To investigate the possibility of small-scale *ATP2A2* mutations, we PCR-amplified exonic sequences from patient cDNA or genomic DNA samples. Initial RT-PCR analyses identified three families (Ox-F15, Ox-S1 and Ox-F4) in which affected members gave aberrant-sized products indicative of intra-exonic deletions or insertions (data not shown). We followed up by comprehensive mutation screening in affected individuals in various families and sporadic patients using conformation-sensitive gel electrophoresis (CSGE) or single strand conformation polymorphism (SSCP) analysis, and subsequent sequencing of aberrant amplification products. We report 13 different *ATP2A2* mutations in affected individuals (Table 2, Fig. 3).

These mutations were not detected in over 50 British control individuals, indicating that these mutations are not likely to be neutral polymorphisms. The mutations predict aberrant splicing, premature translation termination, non-conservative missense mutations and an intra-exonic in-frame duplication. The intra-exonic duplication observed in family Ox-F15, 91ins57, spans nt 35–91 of the cDNA sequence[11] and predicts a tandem duplication of aa V12–L32. Deletions include an in-frame deletion (2102del36) which removes the sequence encoding aa G701–K712 (Fig. 3), and four small deletions which occur in various exons and have the potential for producing a frameshift (Fig. 3). Another deletion, 1418delCA, which removes the last two nucleotides of exon 11, leads to in-frame skipping of exon 11 (encoding A430–S473) in patient Ox-F4 (Fig. 3). A nonsense mutation (Q108X) at the last codon of exon 4 causes in-frame skipping of exon 4 (encoding V74–Q108) in patient Ox-S1. A splice-site mutation in NCL-Cx (544+1G→A) occurs at the guanine of the conserved GT dinucleotide in the donor splice site of intron 6, and although lack of access to further patient samples precluded follow-up at the transcript level, this mutation probably alters splicing of exon 6

**Table 2 • *ATP2A2* mutations in patients with DD**

| Family/ patient | Location | Mutation[a] | Nucleotide change[b] | Consequence | Protein domain | Verification method |
|---|---|---|---|---|---|---|
| NCL-B11 | exon 1 | G23E | 68G→A | missense | upstream stalk 1 | *Alu*I |
| Ox-F15 | exon 1 | 91ins57 | AGAAGC→AGATGC...AGAAGC | in-frame insertion | upstream stalk 1 | 2% agarose gel |
| Ox-S1 | exon 4 | Q108X | 322C→T | in-frame exon skipping | M1, loop, M2 | *Bsp*MI |
| NCL-A39 | exon 5 | 433delAT | GACATAGT→GACAGT | frameshift (PTC+3 aa) | β sheet | *Alw*NI |
| NCL-Cx | intron 6 | 544+1g→a | CAGgt→CAGat | altered splicing | β sheet | SSCP |
| Ox-F11 | exon 8 | T357K | 1070C→A | missense | phosphorylation | CSGE |
| NCL-B4 | exon 10 | 1220delAT | AGTATGAT→AGTGAT | nonsense | phosphorylation | *Bst*XI, *Xcm*I |
| Ox-F4 | exon 11 | 1418delCA | ACTCAgt→ACTgt | in-frame exon skipping | phosphorylation | *Dde*I |
| Ox-F36 | exon 12 | S495L | 1484C→T | missense | phosphorylation | CSGE |
| NCL-B37 | exon 14 | 2017delC | GCCCGCT→GCCGCT | frameshift (PTC+14 aa) | ATP binding | SSCP |
| Ox-F22 | exon 15 | 2102del36 | CTGGC...AGCCG→CTGCCG | in-frame deletion | hinge | *Mbo*II |
| Ox-F19 | exon 15 | G749R | 2245G→A | missense | stalk 5 | CSGE |
| Ox-F13 | exon 19 | 2790del8 | CATCTGGCTCGTGG→CATTGG | frameshift (PTC+47 aa) | M9 | CSGE |

[a]Numbering of the amino acids refers to the SERCA2a peptide sequence. [b]Numbering of the nucleotides refers to *ATP2A2a* cDNA sequence, with the first nucleotide of ATG initiation codon as 1. Bases in exons are denoted by uppercase letters; bases in introns by lowercase letters; and altered bases are underlined. PTC+n aa, premature termination codon at n amino acid downstream of the mutation; M, transmembrane domain; the TGA stop codon caused by 1220delAT is boxed.

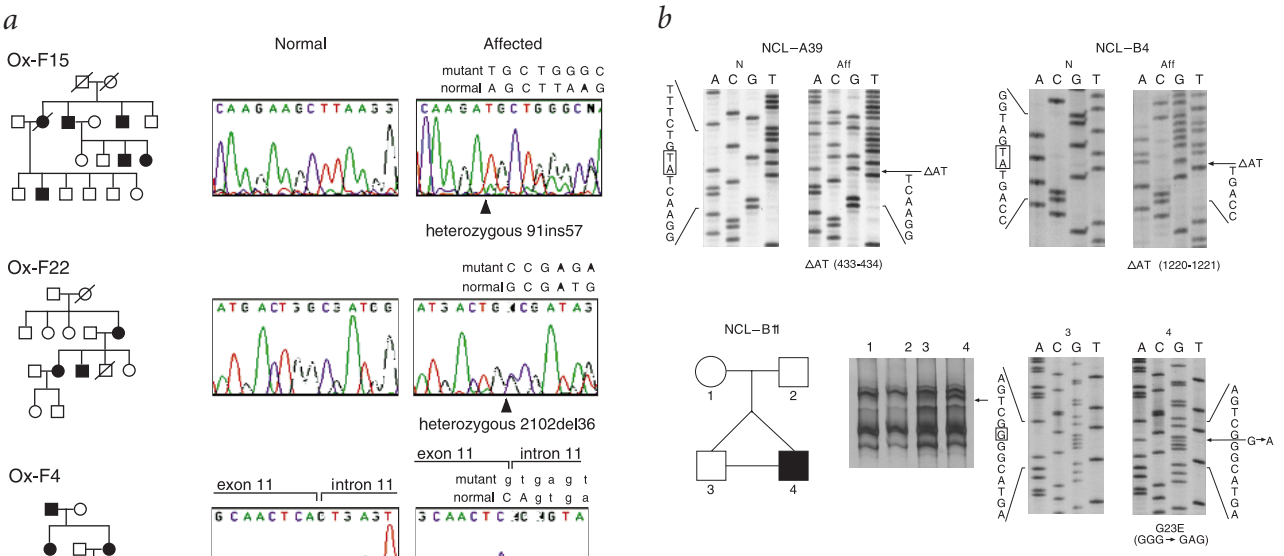


**Fig. 3** Identification of *ATP2A2* mutations in familial and sporadic patients with DD. ***a***, Analysis of familial cases. Affected individuals are indicated by filled symbols, unaffected individuals by open symbols. The affected status of first-generation parents in families Ox-F15 and Ox-F11 is unknown. Direct PCR sequencing of *ATP2A2* mutations from genomic DNA is shown for patients from families Ox-F15, Ox-F22 and Ox-F4. The presence of a heterozygous insertion in patient Ox-F15 (91ins57) and heterozygous deletions in patients Ox-F22 (2102del36) and Ox-F4 (1418delCA) results in the superimposition of the normal and mutant alleles downstream of the mutations. Arrowheads indicate the position of *ATP2A2* mutations. In patient Ox-F4, sequence analysis of the RT-PCR product of smaller size obtained with cDNA primers revealed the in-frame skipping of exon 11 in *ATP2A2*, encoding aa A430–S473. ***b***, Analysis of sporadic cases NCL-A39, NCL-B4 and NCL-B11. NCL-B11 comprises two identical twins, of which only one is affected. Direct PCR sequencing of genomic DNA from patients NCL-A39 and NCL-B4 shows the mixture of normal and mutant alleles downstream of the heterozygous 2-bp deletion (arrows; ΔAT433–434 and ΔAT1220–1221). SSCP analysis in family NCL-B11 shows patient-specific SSCP band revealed with DNA primer set 1. Sequence analysis of *ATP2A2* in patient 4 (affected twin) shows a *de novo* G→A mutation changing glycine 23 into glutamic acid (G23E). This mutation was absent in the unaffected twin and parents of patient 4.

and has a deleterious effect on expression of *ATP2A2*. Finally, four non-conservative missense mutations were identified: G23E, T357K, S495L and G749R (Table 2). Each of these missense mutations results in non-conservative amino acid substitutions at positions highly homologous between species. These changes are likely to affect gene expression and it is noteworthy that the first of these, G23E, has occurred *de novo* in a sporadic patient, NCL-B11. This affected individual has a genetically identical twin (as confirmed by typing at a series of highly polymorphic marker loci used routinely in zygosity testing; data not shown) who, like the two parents, is unaffected. SSCP analysis of the family members identified a variant in exon 1 in the affected twin which was absent in the unaffected twin and both parents (Fig. 3*b*). Sequencing revealed a G→A substitution at nt 68 in the affected twin, which changes glycine 23 into glutamic acid (Fig. 3*b*). This mutation (G23E) was absent from the unaffected identical twin and in both parents, as confirmed by typing for mutant-specific restriction fragments following the creation of a novel *Alu*I site (data not shown).

## Discussion

The cause of DD has eluded clinicians and scientists for many years. Linkage analysis in affected families mapped the DD locus to chromosome 12q23–24.1. We refined the critical region to less than 1 cM and identified 12 genes in the critical region. Seven of these genes were screened for mutations. *ATP2A2*, which is highly expressed in keratinocytes, was found to be mutated in both inherited and sporadic cases.

***ATP2A2* mutations disrupt essential functional domains.** The *ATP2A2* mutations that we describe occur in regions encoding domains that are highly conserved during evolution and are likely to be critical for normal function of SERCA2. Human SERCA2 exhibits extensive similarity (99–99.6% identity at the amino acid level) to rabbit, pig, rat and cat SERCA2. All known SERCA2 proteins from different species show 100% homology in the β strand, transmembrane and stalk domains, and high amino acid conservation in the phosphorylation (97.8%), ATP-binding (97.7%) and hinge (98.3%) domains (Fig. 4). The deduced amino acid sequence of human SERCA2 is also highly conserved among the other human SERCA proteins, showing 82 and 76% identity with SERCA1 and SERCA3, respectively.

A structural model of SERCA pumps has been proposed on the basis of their amino acid sequences, site-directed mutagenesis experiments and modelling studies[12,18,19] (Fig. 4). The mutations that we have described are scattered throughout the gene and alter functional domains of SERCA2 which have a role in $Ca^{2+}$ transport across the endoplasmic reticulum (ER) membrane (Fig. 4, Table 2). Mutations 433delAT, 1220delAT and 2017delC predict severely truncated proteins missing at least three of the transmembrane domains M5, M6 and M8, which contain $Ca^{2+}$-binding sites[20]. A fourth frameshift mutation, 2790del8bp, at the C-terminal region of the molecule alters the transmembrane domains M9 and M10 and may affect anchorage to the ER membrane. Other defects predict the in-frame insertion or deletion of large sequences in functional domains that are strongly con-

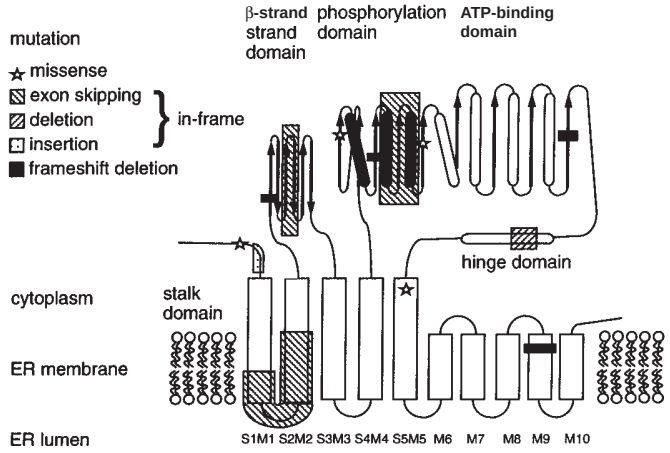


**Fig. 4** Model of the human SERCA2 polypeptide and mutations identified in patients with DD. The predicted secondary structure includes three globular cytoplasmic domains separated by a stalk sector from the transmembrane part of the molecule. The cytoplasmic domain contains a β-strand, a phosporylation and an ATP-binding domain. A hinge region links the ATP-binding domain to stalk sector 5. The transmembrane region includes ten transmembrane coiled-coil helices, four of which contain $Ca^{2+}$-binding sites[20] (M4, M5, M6 and M8). *SERCA2* mutations identified in DD patients are indicated. S1–S5 refer to stalk sectors and M1–M10 refer to transmembrane helices 1–10 (adapted from ref. 40; permission for reproduction has been obtained from D.H. MacLennan and *J. Biol. Chem.*).

served. The in-frame insertion 91ins57 affects a region that contains a signal for ER localization[21]. Abnormal splicing resulting from mutations Q108X, 544+1G→A and 1418delCA disrupts the first and second transmembrane domains (M1, M2), the cytoplasmic β-strand domain, including a highly conserved TGE motif involved in transduction of the energy of ATP hydrolysis to $Ca^{2+}$ transport and the phosphorylation domain. An in-frame deletion (2102del36) alters the highly conserved hinge region among cation-transport ATPases. The missense mutations that we have identified predict changes in the charge and biochemical properties of highly conserved amino acid residues. The G23E mutation replaces a hydrophobic amino acid residue by an acidic one in the hydrophobic potential signal-peptide region of the molecule. Mutations T357K and S495L occur in the phosporylation domain; T357K is located in the consensus motif ICSDKTGTLT near aspartate 351, which undergoes phosphorylation in all ATPases. G749R introduces a positive charge adjacent to two negatively charged glutamic acid residues in the stalk 5 segment of the molecule.

**SERCA2 and cell-to-cell adhesion in the epidermis.** Our results provide the first evidence that SERCA2 influences adhesion between keratinocytes and cellular differentiation in the epidermis. Desmosomes are the prime cell-cell adhesion junctions in the epidermis[22–24]. Their components include desmosomal cadherins (desmogleins and desmocollins), plaque proteins (desmoplakins and plakoglobin) and plaque-associated proteins such as plakophilin 1. By analogy with classical cadherins, adhesion is thought to involve homophilic interactions between extracellular domains of desmosomal cadherins[25]. Recent work suggests that desmoplakins, plakoglobin and plakophilin 1 link cytoplasmic domains of desmosomal cadherins to the keratin intermediate filaments network[26]. The assembly of desmosomes in epithelial cells *in vitro* is initiated through an increase in the extracellular $Ca^{2+}$ concentration[27,28], but variations in intracellular $Ca^{2+}$ are also thought to be important in regulating epithelial cell-to-cell adhesion[24]. Consistent with this notion is the observation that changes in intracellular $Ca^{2+}$ concentration occur at sites of junction assembly of epithelial cells[29]. Evidence for the role of SERCA in the formation of desmosomes has been provided by *in vitro* studies with thapsigargin (TG), a selective inhibitor of the SERCA pumps. TG blocks reuptake of $Ca^{2+}$ from the cytosol, thus depleting $Ca^{2+}$ stores in the ER (ref. 30). Epithelial cells cultured in the presence of TG show abnormal intercellular junction formation[15]. Treatment with TG delays the transport of desmoplakin to the plasma membrane, indicating a role for $Ca^{2+}$-dependent signalling pathway in sorting of desmoplakin[15]. Further support for a role of SERCA in protein trafficking comes from studies in yeast in which mutations in *PMR1* encoding a $Ca^{2+}$-ATPase pump, cause release of incompletely processed secretory proteins from the ER(ref. 31). Partial inhibition of SERCA pumps with low doses of TG alters the oscillation pattern of $Ca^{2+}$ spikes in the cytosol[32]. It is likely that patients with DD who are heterozygous for a mutated *ATP2A2* allele will have only partial deficiency of the SERCA2 pump. By analogy with the consequences of partial inhibition of SERCA pumps *in vitro*, we postulate that DD patients will exhibit altered $Ca^{2+}$ signalling in epidermal cells, possibly through the alteration of cytosolic $Ca^{2+}$ oscillations. This may trigger a cascade of events involving the phosphorylation of target proteins, the regulation of gene transcription[16,33] or the transport of desmosomal proteins to the plasma membrane, resulting in impaired desmosome assembly or altered anchorage of cytokeratin filaments to the desmosomal plaque.

**Proposed mechanism for dominant inheritance.** Mutations in $Ca^{2+}$-ATPase pumps have been described in two diseases, but unlike DD, both are recessive. Mutations in *ATP2A1* underlie some forms of Brody disease, a rare recessive disorder of skeletal muscle in which relaxation of skeletal muscle is impaired[19,34]. Mutations in *Atp2b2*, encoding a plasma membrane $Ca^{2+}$-ATPase type 2 pump, have been identified in deafwaddler mice, which are deaf and display vestibular/motor imbalance[35]. We believe that our findings represent the first description of a dominant phenotype caused by a mutation in a $Ca^{2+}$-ATPase pump. The mutations in DD patients are family specific and predict a wide range of defects. They vary from premature termination codons, which are likely to lead to reduction in mutated *ATP2A2* mRNA through 'nonsense-mediated mRNA decay' as reported for other genes[36], to polypeptides lacking the sequence encoded by an exon or carrying a single amino acid substitution. As SERCA does not require oligomerization to provide a functional channel[37], the mutations are unlikely to have a dominant-negative effect. We suggest that mutations in *ATP2A2* produce a dominant DD phenotype through haploinsufficiency. Mutations disrupt important domains of the molecule and are likely to result in complete or partial loss of function of the mutated pumps. Compensation by the normal SERCA2 pumps and by other systems involved in intracellular $Ca^{2+}$ homeostasis is not sufficient in adult skin and results in abnormal $Ca^{2+}$ signalling in the epidermis. Haploinsuf-

ficiency of the desmoplakin gene has recently been reported in dominant striate palmoplantar keratoderma, illustrating a distinct mechanism involving genetic alteration of a structural desmosomal component in epidermal diseases[38].

Our findings also suggest possible new mechanisms underlying acantholytic skin disorders such as Hailey-Hailey[39] (benign familial pemphigus) and Grover disease[40] (transient acantholytic dermatosis). Further functional studies are needed to understand the mechanisms by which altered SERCA2 function leads to epidermal acantholysis and dyskeratosis. Similarly, such studies could provide insight into the late onset, focal cutaneous distribution, aggravation by external factors and phenotypic variability of the disease. The findings described here provide insights into the role of $Ca^{2+}$ signalling in maintaining epidermal integrity.

## Methods

**Patients and families.** We studied eight unrelated British families and five sporadic cases. The diagnosis was established by a dermatologist (S.B. or C.S.M.) on the basis of clinical examination and was confirmed by histological examination of a skin biopsy in at least one member of each family. Diagnostic clinical features included keratotic papules or plaques on the trunk, a nail dystrophy and/or palmar pits. Family NCL-B11 comprises identical twins, only one of whom is affected with DD. This study was approved by the local Ethics Committee. Blood samples and skin biopsies were obtained after patients had given informed consent.

**Mutation analysis.** Genomic DNA was extracted from peripheral blood leucocytes using standard procedures. We designed primers to amplify all 21 exons and flanking intronic splice sites of *ATP2A2* from genomic DNA (primer sequences available on request). Alternatively, we extracted total RNA from immortalized lymphocyte cell lines using Trizol (Life Technologies). First strand cDNA was synthesized from RNA (5 μg) with Superscript reverse transcriptase (Life Technologies) and random hexamer primers (Pharmacia Biotech). We amplified the entire coding sequence of *ATP2A2* cDNA using overlapping sets of primers (sequence available on request). We carried out PCR reactions using standard reaction mixes containing magnesium chloride (1.5 mM), except for the PCR reaction to amplify exon 1, which was supplemented with betane (2 M). After an initial denaturation step at 94 °C for 4 min, 35 cycles of amplification consisting of 30–60 s at 94 °C, 30–60 s at the optimally determined annealing temperature (51–67 °C) and 30–60 s at 72 °C were performed. RT-PCR products were run on 2% agarose gels for detection of splicing abnormalities. We screened genomic and RT-PCR products for mutations by either CSGE or SSCP. For CSGE analysis, the formation of heteroduplexes was enhanced by heating PCR or RT-PCR products to 98 °C for 5 min, followed by 68 °C for 1 h. Sample (5 μg) was loaded onto a gel containing 10% polyacrylamide, 15% formamide, 10% ethylene glycol and 0.5% glycerol-tolerant buffer (USB) and were subjected to electrophoresis at 500 V for 16 h. The gel was stained with ethidium bromide and visualized under an ultraviolet transilluminator. SSCP gels consisted of 1×MDE solution (FMC), 5% glycerol, 0.6×TBE buffer and were run at 300 V overnight. Following electrophoresis, gels were fixed in ethanol/acetic acid and stained using silver nitrate, following standard methods. We sequenced PCR or RT-PCR fragments showing aberrant migration patterns or extra bands in forward and reverse orientations. PCR or RT-PCR products that showed a single band on 2% agarose gel were purified directly using a QIAquick PCR purification kit (Qiagen). PCR or RT-PCR products that showed more than one band were run in low melting point agarose gel. We separated and gel-purified the bands using QIAEX gel purification kit (Qiagen). We sequenced the purified products using the ABI PRISM AmpliTaq-reaction dye terminator cycle-sequencing kit (PE Applied Biosystems) and an Applied Biosystems model 373A automated sequencer or a Thermosequenase $^{33}$P-ddNTP terminator cycle sequencing kit (Amersham) according to the manufacturer's instructions. We subcloned PCR products that showed 'superimposed' sequences into pGEM-T vector (Promega) or the TA subcloning kit (Invitrogen) and sequenced mutiple subclones.

**Northern-blot analysis.** We generated PCR probes specific for the 3′ UTR of *ATP2A2a (D12S2026)* and *ATP2A2b (D12S1965)*. After purification using QIAquick PCR purification kit (Qiagen), these probes were radiolabelled with [$^{32}$P] αdCTP using the Megaprime DNA labelling system (Amersham) and separated from unincorporated nucleotides with ProbeQuant G-50 Micro Columns (Pharmacia Biotech). We hybridized the *ATP2A2a* and *ATP2A2b*-specific probes to human keratinocyte total RNA (30 μg) northern blots and to multiple-tissue northern blots (human I, Clontech) in Express-Hyb solution (Clontech), followed by washing according to the manufacturer's instructions.

**GenBank accession numbers.** Human: *ATP2A1*, U96781 and P11719; *ATP2A2a*, M23115 and P16614; *ATP2A2b*, M23114 and P16615; *ATP2A3*, Q93084; *ARC21*, AF006086 and P43490; *RPL31*, X15940 and P12947; *PPM2C*, H73417; *PPP1CC*, X74008 and P36873; *RPL29*, U49083 and P47914; gene similar to cytoskeletal proteins, AI23295; *MYL2*, M21812; PAC 305I20, AC006088. Other species: rabbit *Atp2a2*, P04192; pig *Atp2a2*, P11606; rat *Atp2a2*, P11508; cat *Atp2a2*, Q00779; pig *GLTP*, P17403; yeast *FET5*, U80218; yeast *PEP11*, P38759; yeast *PMR1*, M25488.

### Acknowledgements

*We thank the clinicians and the families who participated; R. Cox and E. Levy for their contribution in the physical mapping and cytogenetic parts of the project; R. Gibbs for the freely available sequence from the NIH-funded Human Genome Sequencing effort at the Baylor College of Medicine Human Genome Sequencing Center (BCM-HGSC); and J. Bell for support and encouragement. A.S. has a fellowship from the Royal Thai Government and the faculty of Medicine, Ramathibodi Hospital, Mahidol University; S.M. had a Wellcome Trust prize studentship; A.P.M. is a Wellcome Principal Research Fellow; A.H. held a Wellcome Trust and an EC research fellowship. S.C. was supported by a Wellcome Trust Project Grant awarded to T.S., C.S.M. and J.R.; V.R.-P. holds an EC fellowship. The work in Cardiff was supported by grants from the Wellcome Trust. N.C. is a Wellcome Senior Research Fellow.*

Received 30 December 1998; accepted 4 February 1999.

1. Burge, S. & Wilkinson, D.J. Darier-White disease: a review of the clinical features in 163 patients. *J. Am. Acad. Dermatol.* **27**, 40–50 (1992).
2. Munro, C.S. The phenotype of Darier's disease: penetrance and expressivity in adults and children. *Br. J. Dermatol.* **127**, 126–130 (1992).
3. Burge, S. & Garrod, D.R. An immunohistological study of desmosomes in Darier's disease and Hailey-Hailey disease. *Br. J. Dermatol.* **124**, 242–251 (1991).
4. Craddock, N. *et al.* The gene for Darier's disease maps to chromosome 12q23–q24.1. *Hum. Mol. Genet.* **2**, 1941–1943 (1993).
5. Bashir, R. *et al.* Localisation of a gene for Darier's disease. *Hum. Mol. Genet.* **2**, 1937–1939 (1993).
6. Carter, S.A. *et al.* Linkage analyses in British pedigrees suggest a single locus for Darier disease and narrow the location to the interval between D12S105 and D12S129. *Genomics* **24**, 378–382 (1994).
7. Ikeda, S. *et al.* Localization of the gene for Darier disease to a 5-cM interval on chromosome 12q. *J. Invest. Dermatol.* **103**, 478–481 (1994).
8. Parfitt, E. *et al.* The gene for Darier's disease maps between D12S78 and D12S79. *Hum. Mol. Genet.* **3**, 35–38 (1994).
9. Wakem, P. *et al.* Localization of the Darier disease gene to a 2-cM portion of 12q23–24.1. *J. Invest. Dermatol* **106**, 365–367 (1996).
10. Monk, S. *et al.* Refined genetic mapping of the Darier locus to a <1-cM region of chromosome 12q24.1, and construction of a complete, high-resolution P1 artificial chromosome/bacterial artificial chromosome contig of the critical region. *Am. J. Hum. Genet.* **62**, 890–903 (1998).
11. Lytton, J. & MacLennan, D.H. Molecular cloning of cDNAs from human kidney coding for two alternatively spliced products of the cardiac $Ca^{2+}$-ATPase gene. *J. Biol. Chem.* **263**, 15024–15031 (1988).
12. MacLennan, D.H., Brandl, C.J., Korczak, B. & Green, N.M. Amino-acid sequence of a $Ca^{2+}$ + $Mg^{2+}$-dependent ATPase from rabbit muscle sarcoplasmic reticulum, deduced from its complementary sequence. *Nature* **316**, 696–700 (1985).
13. Pozzan, T., Rizzuto, R., Volpe, P. & Meldolesi, J. Molecular and cellular physiology of intracellular calcium stores. *Physiol. Rev.* **74**, 595–636 (1994).
14. Missiaen, L. *et al.* $Ca^{2+}$ extrusion across plasma membrane and $Ca^{2+}$ uptake by intracellular stores. *Pharmacol. Ther.* **50**, 191–232 (1991).
15. Stuart, R.O., Sun, A., Bush, K.T. & Nigam, S.K. Dependence of epithelial intercellular junction biogenesis on thapsigargin-sensitive intracellular calcium stores. *J. Biol. Chem.* **271**, 13636–13641 (1996).
16. Berridge, M.J., Bootman, M.D. & Lipp, P. Calcium—a life and death signal. *Nature* **395**, 645–648 (1998).
17. Baba-Aissa, F., Raeymaekers, L., Wuytack, F., Dode, L. & Casteels, R. Distribution and isoform diversity of the organellar $Ca^{2+}$ pumps in the brain. *Mol. Chem. Neuropathol.* **33**, 199–208 (1998).
18. Brandl, C.J., Green, N.M., Korczak, B. & MacLennan, D.H. Two $Ca^{2+}$ ATPase genes: homologies and mechanistic implications of deduced amino acid sequences. *Cell* **44**, 597–607 (1986).
19. MacLennan, D.H., Rice, W.J., Odermatt, A. & Green, N.M. Structure-function relationships in the $Ca^{2+}$-binding and translocation domain of SERCA1: physiological correlates in Brody disease. *Acta Physiol. Scand.* **643** (suppl.), 55–67 (1998).
20. Clarke, D.M., Loo, T.W., Inesi, G. & MacLennan, D.H. Location of high affinity $Ca^{2+}$-binding sites within the predicted transmembrane domain of the sarcoplasmic reticulum $Ca^{2+}$-ATPase. *Nature* **339**, 476–478 (1989).
21. Carafoli, E., Garcia-Martin, E. & Guerini, D. The plasma membrane calcium pump: recent developments and future perspectives. *Experientia* **52**, 1091–1100 (1996).
22. Burge, S. Cohesion in the epidermis. *Br. J. Dermatol.* **131**, 153–159 (1994).
23. Garrod, D.R., Chidgey, M.A.J. & North, A.J. Desmosomes: differentiation, development, dynamics and disease. *Curr. Opin. Cell Biol.* **8**, 670–678 (1996).
24. Burdett, I.D.J. Aspects of the structure and assembly of desmosomes. *Micron* **29**, 309–328 (1998).
25. Koch, P.J. & Franke, W.W. Desmosomal cadherins: another growing multigene family of adhesion molecules. *Curr. Opin. Cell Biol.* **6**, 682–687 (1994).
26. Smith, E.A. & Fuchs, E. Defining the interactions between intermediate filaments and desmosomes. *J. Cell Biol.* **141**, 1229–1241 (1998).
27. Watt, F.M., Mattey, D.L. & Garrod, D.R. Calcium-induced reorganization of desmosomal components in cultured human keratinocytes. *J. Cell Biol.* **99**, 2211–2215 (1984).
28. Duden, R. & Franke, W.W. Organization of desmosomal plaque proteins in cells growing at low calcium concentrations. *J. Cell Biol.* **107**, 1049–1063 (1988).
29. Nigam, S.K., Rodriguez-Boulan, E. & Silver, R.B. Changes in intracellular calcium during the development of epithelial polarity and junctions. *Proc. Natl Acad. Sci. USA* **89**, 6162–6166 (1992).
30. Lytton, J., Westlin, M. & Hanley, M.R. Thapsigargin inhibits the sarcoplasmic or endoplasmic reticulum $Ca^{2+}$-ATPase family of calcium pumps. *J. Biol. Chem.* **266**, 17067–17071 (1991).
31. Rudolph, H.K. *et al.* The yeast secretory pathway is perturbed by mutations in PMR1, a member of a $Ca^{2+}$ ATPase family. *Cell* **58**, 133–145 (1989).
32. Petersen, C.C.H., Petersen, O.H. & Berridge, M.J. The role of endoplasmic reticulum calcium pumps during cytosolic calcium spiking in pancreatic acinar cells. *J. Biol. Chem.* **268**, 22262–22264 (1993).
33. Dolmetsch, R.E., Xu, K. & Lewis, R.S. Calcium oscillations increase the efficiency and specificity of gene expression. *Nature* **392**, 933–936 (1998).
34. Odermatt, A. *et al.* Mutations in the gene encoding SERCA1, the fast-twitch skeletal muscle sarcoplasmic reticulum $Ca^{2+}$ ATPase, are associated with Brody disease. *Nature Genet.* **14**, 191–194 (1996).
35. Street, V.A., McKee-Johnson, J.W., Fonseca, R.C., Tempel, B.L. & Noben-Trauth, K. Mutations in a plasma membrane $Ca^{2+}$-ATPase gene cause deafness in deafwaddler mice. *Nature Genet.* **19**, 390–394 (1998).
36. Maquat, L.E. When cells stop making sense: effect of non-sense codons on RNA metabolism in vertebrate cells. *RNA* **1**, 453–465 (1995).
37. Lytton, J. & MacLennan, D.H. Sarcoplasmic reticulum. in *The Heart and Cardiovascular System* (ed. Fozzard, H.A.) 1203–1211 (Raven, New York, 1992).
38. Keith, D. *et al.* Haploinsufficiency of desmoplakin causes a striate subtype of palmoplantar keratoderma. *Hum. Mol. Genet.* **8**, 143–148 (1999).
39. Hailey, H. & Hailey, H. Familial benign chronic pemphigus. *Arch. Dermatol.* **39**, 679–685 (1939).
40. Grover, R.W. Transient acantholytic dermatosis. *Arch. Dermatol.* **101**, 426–434 (1970).
41. Toyofuku, T., Kurzydlowski, K., Lytton, J. & MacLennan, D.H. The nucleotide binding/hinge domain plays a crucial role in determining isoform-specific $Ca^{2+}$ dependence of organellar $Ca^{2+}$-ATPases. *J. Biol. Chem.* **267**, 14490–14496 (1992).